

# Compressive Properties of Panels in Reinforced Concrete Core Walls



**N. Minami**  
Giken Corporation, Japan

**T. Nakachi**  
Fukui University of Technology, Japan

**SUMMARY:**

In high-rise buildings with a core wall system, which consists of four L-shaped core walls, the axial load of the core wall is remarkably high under the action of diagonal seismic force. In particular, the area near the corner of L-shaped core walls is subject to high compressive stress and should be reinforced to improve the deformation capacity of the core walls. In this study, compression tests were conducted on rectangular section columns simulating the area near the corner of L-shaped core walls. The results of the compression tests were compared with those of lateral loading tests on wall columns simulating the area near the corner of L-shaped core walls. The comparison showed that the results of compression tests represented the compressive properties of the panel in the core wall.

*Keywords: Reinforced concrete, core wall, deformation capacity, compression test, confining steel*

**1. INTRODUCTION**

Previously, we conducted lateral loading tests on multistory L-shaped reinforced concrete core walls and examined the relationship between the confinement effect of the area near the corner and the deformation capacity of core walls.<sup>1)</sup> We also conducted compression tests on square and rectangular section columns simulating the area near the corner of L-shaped core walls.<sup>2)</sup> In the present study, in order to examine the deformation capacity of core walls, central compression tests and eccentric compression tests were conducted on rectangular section columns simulating the area near the corner of L-shaped core walls. The parameters of the compression tests were the amount of confining steel, the type of concrete confinement and the horizontal pitch of the confining steel. The type of concrete confinement was tie bar and closed reinforcement. The results of eccentric compression tests were compared with those of a lateral loading test on a wall column simulating the area near the corner of L-shaped core walls.

**2. COMPRESSION TESTS**

**2.1 Summary of Tests**

*2.1.1 Test specimens*

The configuration and arrangement of reinforcement in the specimens are shown in Fig. 1. The characteristics of the specimens are listed in Table 1. The physical properties

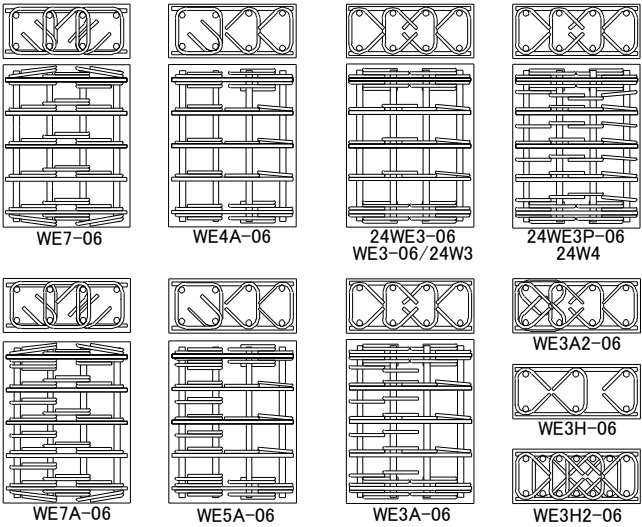


**Fig. 1** Test Specimens

**Table 1** Characteristics of Specimens

Specimen	Fc (N/mm <sup>2</sup> )	Loading	Confining Steel	Vertical Pitch of Confining Steel (mm)
WE0-06	60	Eccentric	Absence	—
WE3-06			Presence	55.0
WE3A-06			Presence	55.0(27.5) *1
WE3A2-06			Presence	55.0
WE3H-06			Presence	55.0
WE3H2-06			Presence	55.0
WE4A-06			Presence	55.0
WE5A-06			Presence	55.0(27.5) *1
WE7-06			Presence	55.0
WE7A-06			Presence	55.0(27.5) *1
24WE0-06	24	Eccentric	Absence	—
24WE1-06			Absence	—
24WE3-06			Presence	55.0
24WE3P-06			Presence	27.5
24W0		Central	Absence	—
24W1			Absence	—
24W3			Presence	55.0
24W4			Presence	27.5

\*1 ( ) : Pitch at Edge Area

of the concrete and reinforcement are listed in Table 2 and Table 3, respectively. Eighteen specimens simulating the panel in the core wall specimens were tested. The specimens had a rectangular cross section measuring 90×210 mm and a height of 270 mm. D10 and D6 deformation bars with yield strength of 402 and 374 N/mm<sup>2</sup> were used for longitudinal and transverse reinforcement, respectively. High-strength bar U5.1 with yield strength of 1368 N/mm<sup>2</sup> was used for the confining steel. The specified design strength of the concrete was 60 and 24 N/mm<sup>2</sup>. The parameters of the compression tests were the amount of confining steel, the type of concrete confinement and the horizontal pitch of the confining steel.

**Table 2** Physical Properties of Concrete

Specimen	Compressive Strength (N/mm <sup>2</sup> )	Young's Modulus (×10 <sup>4</sup> N/mm <sup>2</sup> )	Sprig Strength (N/mm <sup>2</sup> )
Fc 24 Series	23.8	1.83	1.43
Fc 60 Series	66.4	2.98	3.81

**Table 3** Physical Properties of Steel

Bar Size	Yield Strength (N/mm <sup>2</sup> )	Maximum Strength (N/mm <sup>2</sup> )	Young's Modulus (×10 <sup>5</sup> N/mm <sup>2</sup> )	Elongation (%)
D10	402	578	2.07	25.7
D6	374	532	1.90	19.7
U5.1	1368	1491	2.11	9.3

The Fc 60 series comprised ten specimens: WE0-06 to WE7A-06. The vertical pitch of the transverse reinforcement and the horizontal pitch of the longitudinal reinforcement were both 55 mm except for Specimens WE3H-06 and WE3H2-06, for which the horizontal pitch of the longitudinal reinforcement was 82.5 and 27.5 mm, respectively. The vertical pitch of the confining steel at the edge area was 27.5 mm in Specimens WE3A-06, WE5A-06 and WE7A-06, and was 55 mm in the other specimens.

The Fc 24 series comprised eight specimens: 24WE0-06 to 24W4. The vertical pitch of the transverse reinforcement and the horizontal pitch of the longitudinal reinforcement were both 55 mm. The

vertical pitch of the confining steel was 27.5 mm in Specimens 24WE3P-06 and 24W4, and was 55 mm in the other specimens.

### 2.1.2 Test procedure

Figure 2 shows the loading and the measuring system. Test specimens were subjected to monotonic uniaxial compression. The pin support was set at the top of the specimens. The distance of eccentricity  $e$  from the center was 35 mm in the eccentric compression tests. Axial strain was measured by transducer. Measuring length was 165 mm. Strain gages were attached to the confining steel, the transverse reinforcement and the longitudinal reinforcement. The suffix -06 was added to the specimen name in the eccentric compression tests for eccentricity  $e$  of 35 mm ( $e = D/6$ ,  $D = 210$  mm). The attachment position of strain gages at the confining steel was the midpoint of the side.

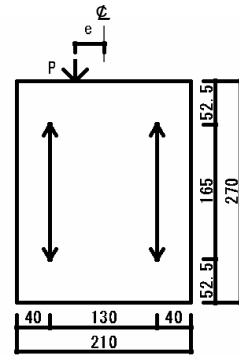


**Fig. 2** Loading and Measuring System

## 2.2 Test Results

### 2.2.1 Maximum moment and maximum stress

Table 4 shows the test results. In the table, the maximum moment is the product of the maximum load and eccentricity. The curvature was found by dividing the difference in strains measured by the two transducers shown in Fig. 2 by the distance between the two transducers. The distance between the two transducers was 190 mm because the axis of the transducer extended 30 mm outside the fixing bolt.

### 2.2.2 Relationship between moment and curvature

Figures 3 and 4 show the relationship between moment and curvature in the case of  $F_c$  60 specimens in the eccentric compression tests. The maximum moment and the curvature at the maximum moment of Specimens WE3A-06 and WE3A2-06 with a larger amount of confining steel at the edge area compared to Specimen WE3-06 confined with tie bars, were larger than that of Specimen WE3-06. That is, the compressive ductility of Specimens WE3A-06 and WE3A2-06 was larger than that of Specimen WE3-06. The ductility of Specimen WE7A-06 with the larger amount of confining steel at the edge area compared to Specimen WE7-06 confined with closed reinforcement, was larger than that of Specimen WE7-06. In a comparison between Specimens WE3H-06 and WE3H2-06, which differed in horizontal pitch of confining steel, the ductility was larger, corresponding to the smaller pitch of the confining steel.

**Table 4** Test Results

Specimen (Eccentric)	Maximum Moment (kN·m)	Curvature at Max. Moment ( $\times 10^{-2}/\text{mm}$ )
WE0-06	25.2	0.0020
WE3-06	27.4	0.0029
WE3A-06	29.6	0.0067
WE3A2-06	28.6	0.0081
WE3H-06	29.6	0.0013
WE3H2-06	36.3	0.0086
WE4A-06	31.1	0.0090
WE5A-06	33.9	0.0125
WE7-06	29.5	0.0267
WE7A-06	38.7	0.0243
24WE0-06	7.8	0.0044
24WE1-06	10.8	0.0039
24WE3-06	14.6	0.0048
24WE3P-06	16.7	0.0092
Specimen (Central)	Maximum Stress (N/mm <sup>2</sup> )	Strain at Max. Stress (%)
24W0	18.3	0.59
24W1	25.5	0.85
24W3	26.4	1.11
24W4	30.3	2.44

Figures 5 and 6 show the relationship between moment and curvature and the relationship between stress and strain in the case of  $F_c$  24 specimens. The ductility of Specimens 24WE3P-06 and 24W4 with the largest amount of confining steel was largest in the central and eccentric compression tests, respectively. The effect of the amount of confining steel on the compressive ductility was similarly shown in both the central and eccentric compression tests.

## 2.3 Analysis Test Results

### 2.3.1 Case of concrete compressive strength 60 N/mm<sup>2</sup>

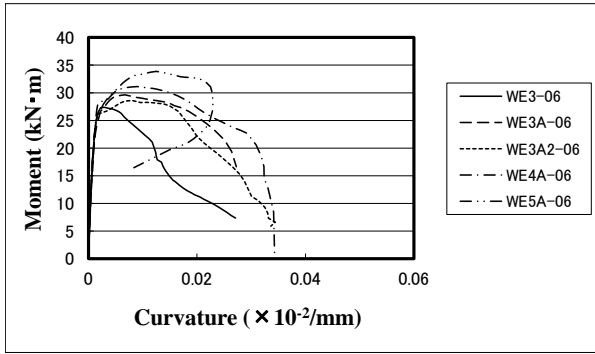


**Fig. 3** Moment versus Curvature Curves (WE3-06, WE3A-06, WE3A2-06, WE4A-06, WE5A-06)

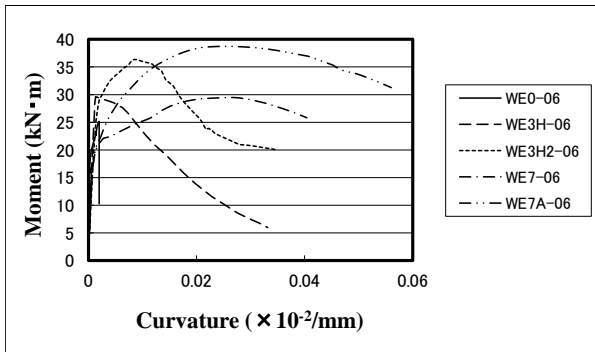


**Fig. 4** Moment versus Curvature Curves (WE0-06, WE3H-06, WE3H2-06, WE7-06, WE7A-06)

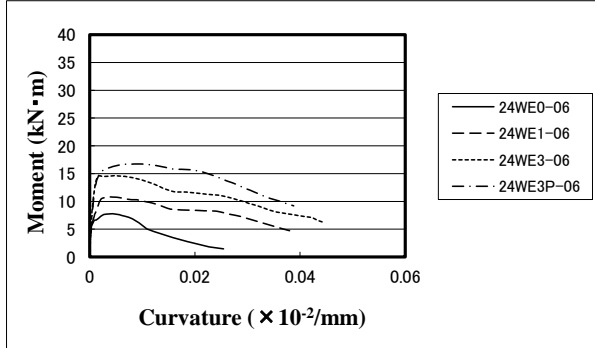


**Fig. 5** Moment versus Curvature Curves (24WE0-06, 24WE1-06, 24WE3-06, 24WE3P-06)

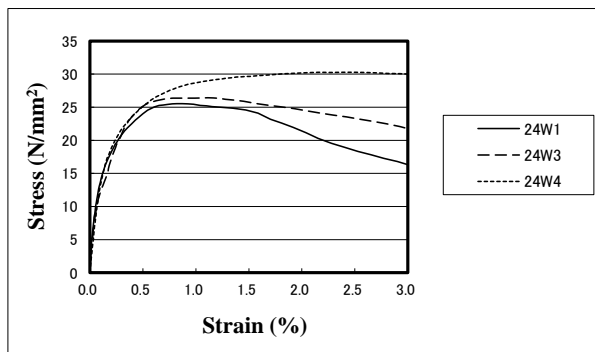
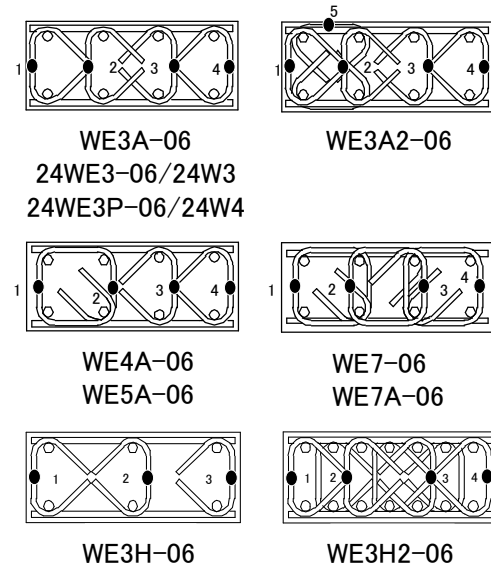


**Fig. 6** Stress versus Strain Curves (24W1, 24W3, 24W4)



● Attachment Position of Strain Gages

**Fig. 7** Attachment Position of Strain Gages

Figure 7 shows the arrangement of reinforcement and the attachment position of strain gages at the confining steel. In the figure, the attachment position of strain gages in the central compression tests was Gage 1 and 2 only. Figure 8 shows the relationship between the strain of the confining steel and the curvature of Specimen WE3A-06. The strain of Gage 1 at the furthest edge area was large during the early stage and decreased after the peak at a curvature. The strain of Gage 2 adjoining Gage 1 became the larger of the two after around the peak of Gage 1 and increased thereafter. It is considered that this tendency shows that the stress of the concrete moved from the furthest edge to the inside area.

Figures 9 and 10 show the relationship between the strain of the confining steel and the curvature of Specimens WE3A2-06 and WE4A-06, respectively. Specimen WE3A2-06 had tie bars added in the longitudinal direction in the cross section at the edge area and Specimen WE4A-06 had closed reinforcement at the edge area. In both specimens, the strain of Gage 1 at the furthest edge area and that of Gage 2 adjoining Gage 1 were large. The strain of Gage 1 and Gage 2 reached a peak at approximately the same curvature, unlike Specimen WE3A-06 in which the peak of Gage 1 and Gage 2 had a lag. It is considered that the confining steel at the area of Gage 1 and Gage 2 had a unified effect on the concrete at the peak, which decreased at the final stage.

Figure 11 shows the relationship between the strain of the confining steel and the curvature of Specimen WE5A-06. In a comparison between Specimen WE4A-06 (Fig. 10) and WE5A-06, the strain of Gage 1 and Gage 2 of both specimens at the curvature of  $0.01 \times 10^{-2}$  was approximately  $4000 \times 10^{-6}$ . Thus, the confining force per confining steel was approximately the same. On the other hand, the amount of confining steel at the edge area of Specimen WE5A-06 was twice that of

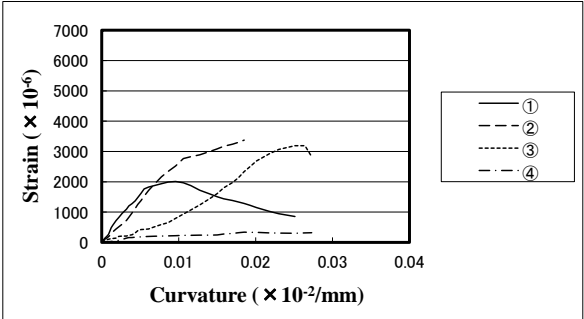


**Fig. 8** Strain of Confining Steel versus Curvature Curves (WE3A-06)

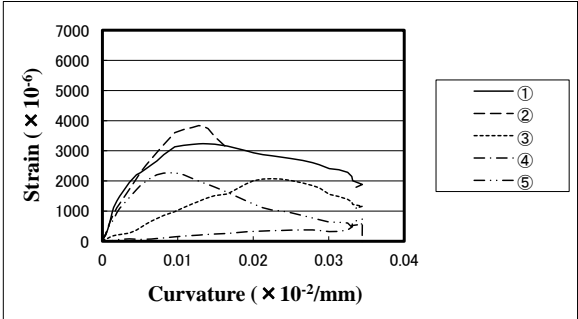


**Fig. 9** Strain of Confining Steel versus Curvature Curves (WE3A2-06)

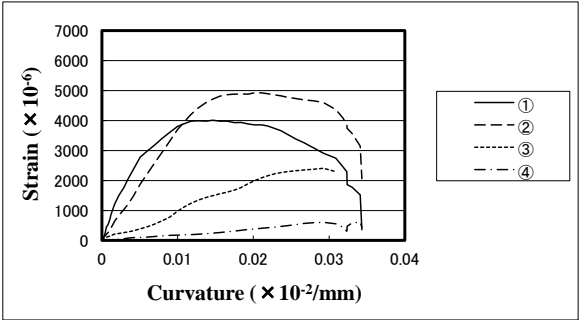


**Fig. 10** Strain of Confining Steel versus Curvature Curves (WE4A-06)

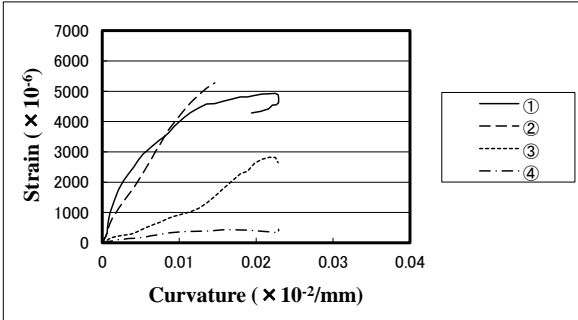


**Fig. 11** Strain of Confining Steel versus Curvature Curves (WE5A-06)

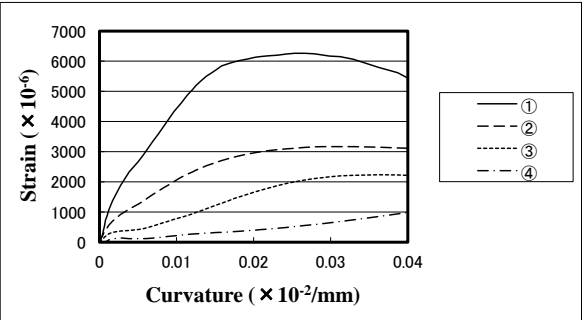


**Fig. 12** Strain of Confining Steel versus Curvature Curves (WE7-06)

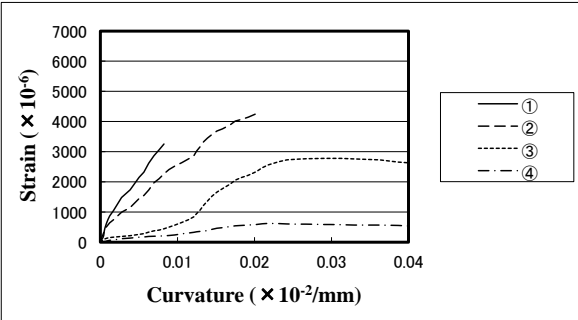


**Fig. 13** Strain of Confining Steel versus Curvature Curves (WE7A-06)

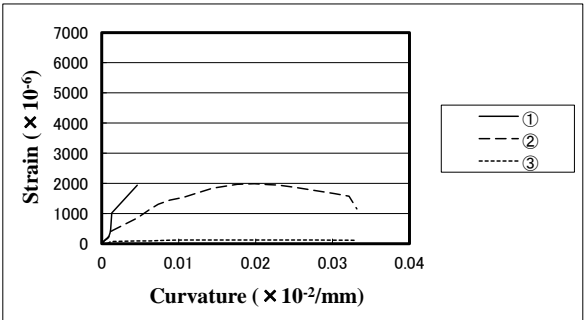


**Fig. 14** Strain of Confining Steel versus Curvature Curves (WE3H-06)

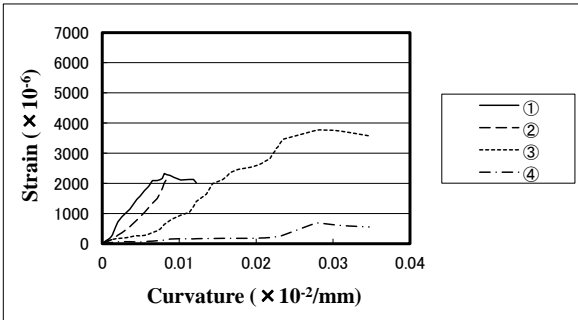


**Fig. 15** Strain of Confining Steel versus Curvature Curves (WE3H2-06)

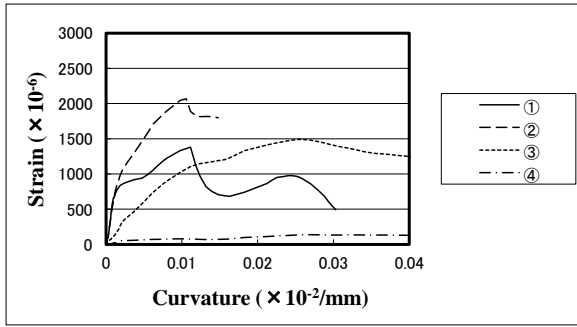


**Fig. 16** Strain of Confining Steel versus Curvature Curves (24WE3-06)

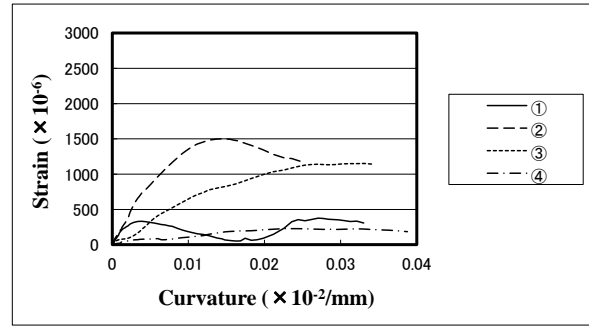


**Fig. 17** Strain of Confining Steel versus Curvature Curves (24WE3P-06)

WE4A-06. As a result, it is considered that the confining force at the edge area of Specimen WE5A-06 was twice that of WE4A-06. This is considered to be the reason why Specimen WE5A-06 was more ductile than Specimen WE4A-06 in the relationship between moment and curvature in Fig. 3.

Figures 12 and 13 show the relationship between the strain of the confining steel and the curvature of Specimens WE7-06 and WE7A-06, respectively. The strain of Gage 1 and Gage 2 of Specimen WE7-06 at the curvature of  $0.005 \times 10^{-2}$  was  $2800 \times 10^{-6}$  and  $1500 \times 10^{-6}$ , respectively. The strain of Gage 1 and Gage 2 of Specimen WE7A-06 at the curvature of  $0.005 \times 10^{-2}$  was  $2800 \times 10^{-6}$  and  $2000 \times 10^{-6}$ , respectively. Thus, the confining force per confining steel was approximately the same. On the other hand, the amount of confining steel at the edge area of Specimen WE7A-06 was twice that of WE7-06. As a result, it is considered that the confining force at the edge area of Specimen WE7A-06 was twice that of WE7-06. This is considered to be the reason why Specimen WE7A-06 was more ductile than Specimen WE7-06 in the relationship between moment and curvature in Fig. 4.

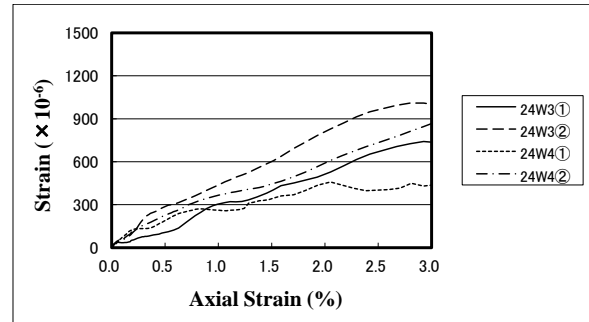


**Fig. 18** Strain of Confining Steel versus Axial Strain Curves (24W3, 24W4)

Figures 14 and 15 show the relationship between the strain of the confining steel and the curvature of Specimens WE3H-06 and WE3H2-06, respectively. The strain of Gage 1 at the curvature of  $0.004 \times 10^{-2}$  was approximately  $2000 \times 10^{-6}$  and  $1500 \times 10^{-6}$  in Specimen WE3H-06 and WE3H2-06, respectively. Thus, the confining force per confining steel in Specimen WE3H-06 was larger than that in Specimen WE3H2-06. On the other hand, the amount of confining steel in the cross section of Specimen WE3H-06 was smaller than that in Specimen WE3H2-06. As a result, it is considered that the confining force at the cross section of Specimen WE3H2-06 was larger than that in Specimen WE3H-06. This is considered to be the reason why Specimen WE3H2-06 was more ductile than Specimen WE3H-06 in the relationship between moment and curvature in Fig. 4.

### 2.3.2 Case of concrete compressive strength $24 \text{ N/mm}^2$

Figures 16 and 17 show the relationship between the strain of the confining steel and the curvature of Specimens 24WE3-06 and 24WE3P-06, respectively. Figure 16 shows the strain in Specimen 24WE3-06 as follows. The strain of Gage 1 at the furthest edge area and that of Gage 2 adjoining Gage 1 were large during the early stage. Thereafter, the strain of Gage 2 became the larger of the two and the strain of Gage 1 and 2 reached a peak at the curvature and then decreased. Figure 17 shows the strain in Specimen 24WE3P-06 as follows. The strain of Gage 1 at the furthest edge area and that of Gage 2 adjoining Gage 1 were large during the early stage. Thereafter, the strain of Gage 2 became the larger of the two and reached a peak at the curvature and then decreased. In a comparison between Specimens 24WE3-06 and 24WE3P-06, the strain of Gage 1, 2 and 3 in Specimen 24WE3P-06 was smaller than that in Specimen 24WE3-06 at all curvatures. On the other hand, the amount of confining steel in Specimen 24WE3P-06 was twice that of 24WE3-06. As a result, it is considered that the

confining force of Specimen 24WE3P-06 was larger than that of 24WE3-06. This is considered to be the reason why Specimen 24WE3P-06 was more ductile than Specimen 24WE3-06 in the relationship between moment and curvature in Fig. 5.

Figure 18 shows the relationship between the strain of the confining steel and the axial strain of Specimens 24W3 and 24W4. In a comparison between Specimens 24W3 and 24W4, the strain of Gage 1 and Gage 2 in Specimen 24W4 was smaller than that in Specimen 24W3 at all axial strain. On the other hand, the amount of confining steel in Specimen 24W4 was twice that of 24W3. As a result, it is considered that the confining force of Specimen 24W4 was larger than that of 24W3, similar to the comparison between Specimens 24WE3-06 and 24WE3P-06 in the eccentric compression tests. This is considered to be the reason why Specimen 24W4 was more ductile than Specimen 24W3 in the relationship between stress and strain in Fig. 6.

### 3. LATERAL LOADING TEST ON CORE WALLS

#### 3.1 Summary of Tests

The configuration and arrangement of reinforcement provided in the specimen are shown in Fig. 19. The physical properties of the concrete and reinforcement are listed in Table 5 and Table 6, respectively.

A one-eighth-scale wall column specimen simulating the area near the corner of L-shaped core walls was tested. The specimen represented the lower three stories of a high-rise building of approximately twenty-five stories. The specimens had rectangular cross sections measuring 90×430 mm, were the flexural type and had a shear span ratio of 2.79. The specified design strength of the concrete was 60 N/mm<sup>2</sup> and the ratio of axial stress to concrete compressive cylinder strength (axial stress ratio) was 0.2. D10 and D6 deformation bars with yield strength of 393 and 372 N/mm<sup>2</sup> were used for longitudinal and transverse reinforcement, respectively. The pitch of the longitudinal and transverse reinforcement was 55 mm, which was identical to that of the specimens of the compression tests. High-strength bar U5.1 with yield strength of 1368 N/mm<sup>2</sup> was used for the confining bars, which was identical to that used in the compression tests. The confining bars were tie bars. The confining bars were arranged up to a height corresponding to the width of the wall column (h: 430 mm). The horizontal and vertical pitch of confining bars was 55 mm, which was identical to that in Specimen WE3-06.

The loading test was the cantilever type, as shown in Figure 20. In the cyclic lateral loading test, the specimen was subjected to lateral forces by a horizontal hydraulic jack connected to the reaction frame. Constant axial loading force was applied by a vertical hydraulic jack over the specimen to represent

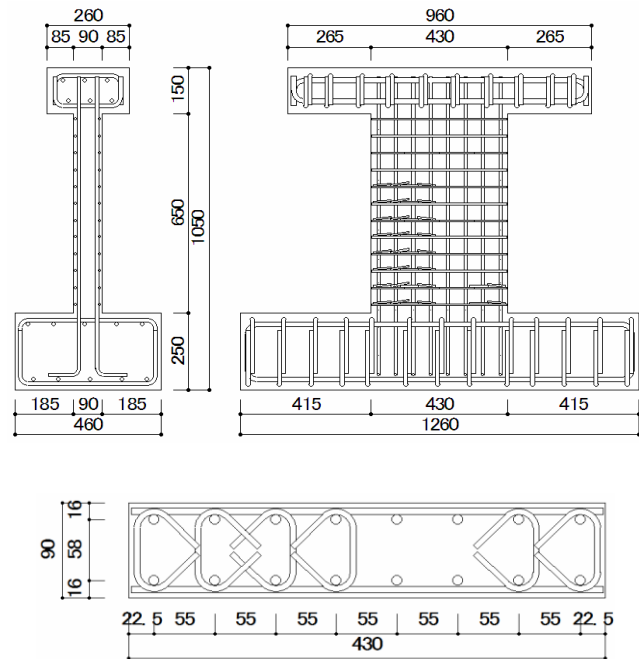


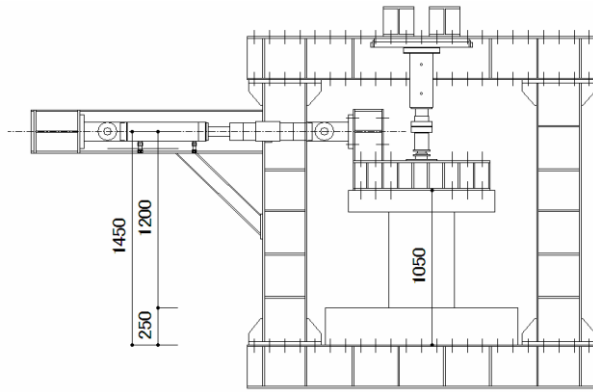
Fig. 19 Test Specimen

Table 5 Physical Properties of Concrete

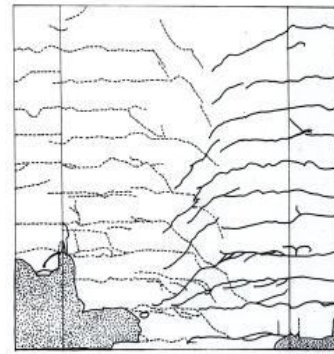
Specimen	Compressive Strength (N/mm <sup>2</sup> )	Young's Modulus (×10 <sup>4</sup> N/mm <sup>2</sup> )	Split Strength (N/mm <sup>2</sup> )
No.1	63.2	2.90	3.40

Table 6 Physical Properties of Steel

Bar Size	Yield Strength (N/mm <sup>2</sup> )	Maximum Strength (N/mm <sup>2</sup> )	Young's Modulus (×10 <sup>5</sup> N/mm <sup>2</sup> )	Elongation (%)
D10	393	568	2.04	25.8
D6	372	524	2.05	25.7
U5.1	1368	1491	2.11	9.3



**Fig. 20** Loading System



**Fig. 21** Crack Pattern

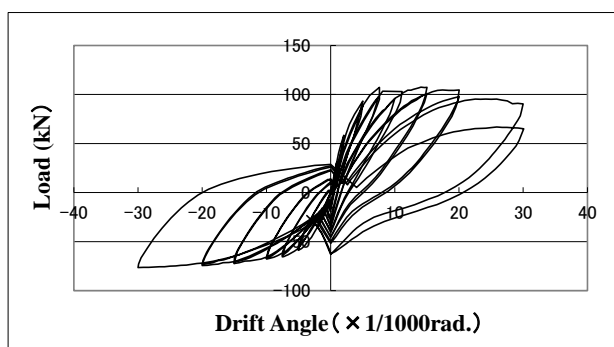


**Fig. 22** Load - Deflection Curve

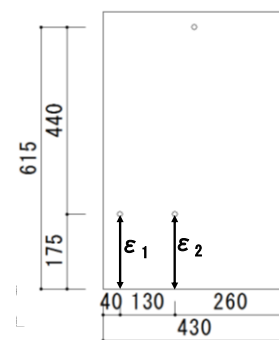


**Fig. 23** Measuring System

the axial stress in the stage of coupling beam yielding at the center core. The axial stress ratio was 0.2 under positive loading for which the corner area of L-shaped core walls is compressive and 30 kN under negative loading, respectively. Loading was controlled by the horizontal drift angle at a height corresponding to the second floor level ( $h$ : 615 mm). The loading was cyclic lateral loading at  $R$  (drift angle) = 1/1000 (rad.) (1 cycle), 2/1000, 5/1000, 7.5/1000, 10/1000, 15/1000, 20/1000 (2 cycle respectively), 30/1000, 40/1000 (1 cycle respectively).

### 3.2 Test Results

The crack pattern of the specimen during the final stage is shown in Fig. 21. Under all negative loading, flexural cracks occurred at the bottom of the specimen. Thereafter, flexural cracks expanded upward and to the middle of the specimen. Under positive loading, the longitudinal reinforcement at the compressive end yielded (yield strain  $1926 \times 10^{-6}$ ) at approximately 5/1000, and the longitudinal reinforcement at the tensile end yielded under negative loading. Under both positive and negative loading, flexural shear cracks occurred at approximately 7.5/1000. The corner area at the bottom appeared to crack vertically and crumbled slightly at 7.5/1000. At the final stage, the specimen crumbled, buckling of the longitudinal reinforcement was observed, and the strength decreased under positive loading. Figure 22 shows the load deflection curves. The maximum strength was 107.3 kN at 15/1000 under positive loading.

## 4. COMPARISON OF RESULTS BETWEEN ECCENTRIC COMPRESSION TESTS AND LATERAL LOADING TEST

The results of the eccentric compression test were compared with the compressive properties at the bottom of the specimen in the lateral loading test. The compression test was performed on Specimen

WE3-06 for which the arrangement of reinforcement was identical to that of Specimen 1 in the lateral loading test. Figure 23 shows the measuring system using the transducer at the bottom of Specimen 1. The measuring length was 175 mm, which was approximately the same as that of the compression test (165 mm). The horizontal distance of the bolts fixing the transducer was 135 mm, which was identical to that of the compression test. The distance between the two transducers was 190 mm because the axis of the transducer extended 30 mm outside the fixing bolt, the same as in the compression test.

Figure 24 shows the vertical strain  $\epsilon_1$  and  $\epsilon_2$  at the peak of the drift angle under positive loading in Specimen 1. Strain  $\epsilon_1$  near the compressive end was approximately proportional to the drift angle. Strain  $\epsilon_2$  was compressive up to around 10/1000, after which it became tensile and increased linearly corresponding to the drift angle. Figure 25 shows the relationship between the drift angle and the curvature calculated from strain  $\epsilon_1$  and  $\epsilon_2$ . The curvature was approximately proportional to the drift angle.

Figure 26 shows the horizontal distribution of strain  $\epsilon_1$  and  $\epsilon_2$  at each drift angle (the second cycle except for 30/1000). Figure 27 shows the horizontal distribution of the vertical strain of Specimen WE3-06 in the eccentric compression test. The vertical strain at the other side of the compressive side was approximately 0 in both Specimen 1 and WE3-06. The neutral axis was 160 to 200 mm from the compressive end in both specimens. Thus, the horizontal distribution in both specimens is considered to be almost the same.

Figures 28 and 29 show the relationship between the strain of the confining steel and the curvature at the area of Specimen 1 and WE3-06 mentioned above. The attachment position of strain gages at the confining steel in Specimen 1 was the same as that of Specimen WE3-06 (Fig. 7) and the height from the bottom in Specimen 1 was 82.5 mm. The tendency of the strain, which was the same in both specimens, was as follows. The strain of Gage 1 at the furthest edge area was large during the early stage and decreased after the peak just before the curvature of  $0.01 \times 10^{-2}$ . The strain of Gage 2 adjoining Gage 1 became the larger of the two after around the peak of Gage 1 and increased thereafter. On the

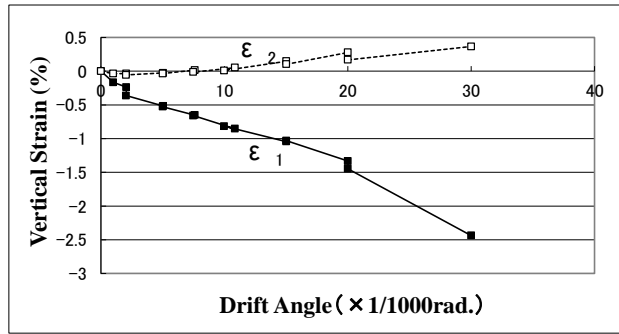


Fig. 24 Vertical Strain versus Drift Angle (No.1)

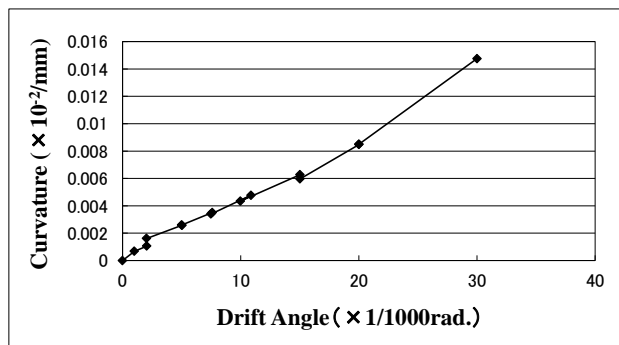


Fig. 25 Curvature versus Drift Angle (No.1)

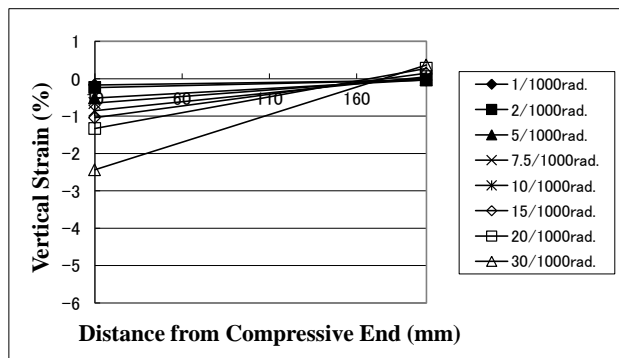


Fig. 26 Horizontal Distribution of Vertical Strain (No.1)

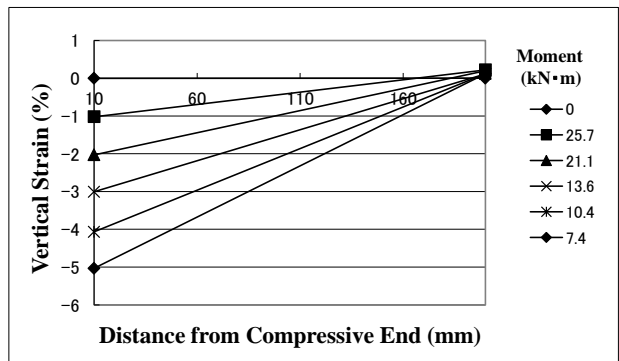
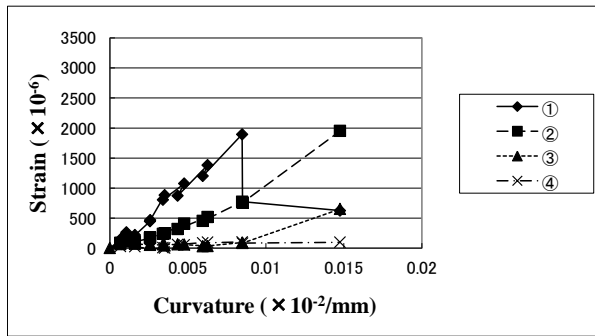
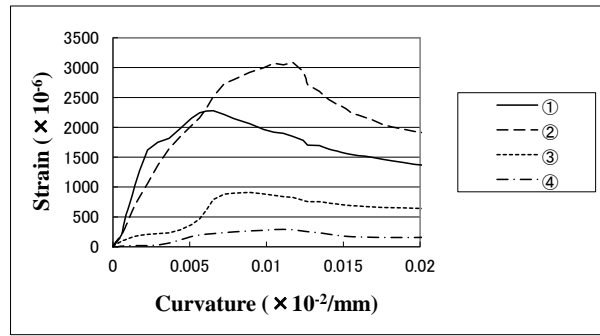


Fig. 27 Horizontal Distribution of Vertical Strain (WE3-06)



**Fig. 28** Strain of Confining Steel versus Curvature Curves (No.1)



**Fig. 29** Strain of Confining Steel versus Curvature Curves (WE3-06)

other hand, the strain at each curvature in Specimen WE3-06 was larger than that in Specimen 1 as a whole and the tendency was obvious at Gage 2 and Gage 3. Based on the horizontal distribution of the vertical strain and the relationship between the strain of the confining steel and the curvature, the compressive properties of Specimen 1 and WE3-06 were considered to be almost the same. Figure 30 shows the relationship between moment and curvature in Specimen WE3-06. From the relationship between the curvature and the drift angle in Specimen 1 shown in Fig. 25, the curvature at 30/1000 was  $0.0148 \times 10^{-2}$ . The circle in Fig. 30 indicates the curvature of  $0.0148 \times 10^{-2}$ . The compressive condition at 30/1000 at which the lateral load decreased largely in the lateral loading test is considered to correspond to the compressive condition in which the moment decreased by 55% from the maximum in the eccentric compression test.

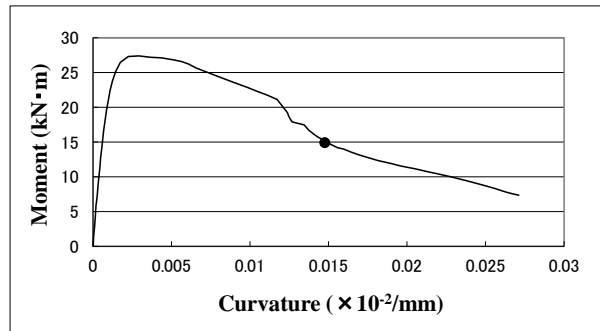


**Fig. 30** Moment versus Curvature Curves (WE3-06)

## 5. CONCLUSIONS

In order to examine the deformation capacity of core walls, central compression tests and eccentric compression tests were conducted on rectangular section columns simulating the area near the corner of L-shaped core walls. The results of eccentric compression tests were compared with that of a lateral loading test on wall column simulating the area near the corner of L-shaped core walls. Major findings are as follows:

- (1) The results of the eccentric compression tests showed the increase in compressive ductility with the increment in amount of confining steel at the edge area and the decrement in horizontal pitch of the confining steel.
- (2) The confining force of the tie-bar-type confining steel moved from the compressive end to the inside area. On the other hand, the closed-type confining force was concentrated in the compressive area.
- (3) A comparison between the compression tests and lateral loading tests showed that the results of the compression tests represented the compressive properties of the compressive area in the core walls.

## REFERENCES

- 1) Nakachi, T., Toda, T., Tabata, K. (1996). Experimental study of deformation capacity of reinforced concrete core walls after flexural yielding. *Proceedings of the 11th World Conference on Earthquake Engineering*, Paper No. 1714.
- 2) Hatakenaka, T., Nakachi, T. (2008). Study on deformation capacity of reinforced concrete core walls after flexural yielding. *Proceedings of the 14th World Conference on Earthquake Engineering*, Paper ID 12-01-0100.